Running head: A NOVEL RESISTANCE-COFERRING MUTATION IN *M. ABSCESSUS*

A single upstream mutation of *whiB7* underlies amikacin and clarithromycin resistance in *Mycobacterium abscessus*

Nathan De Boeck[1,2,3], Cristina Villellas[3,4,#], Estefanía Crespo-Yuste[4,5], Jesús Gonzalo-Asensio[4,5], Peter T. Buckley[3], Kim Thys[3], Cuong Vuong[3], Nacer Lounis[3], Natalie Verstraeten[1,2], Jan Michiels[1,2,#,*]

[1]Center for Microbiology, VIB-KU Leuven, 3001 Leuven, Belgium
[2]Centre of Microbial and Plant Genetics, KU Leuven, 3001 Leuven, Belgium
[3]Communicable Diseases Unit, Janssen Research & Development, LLC, a Johnson & Johnson Company, 2340 Beerse, Belgium
[4]Grupo de Genética de Micobacterias, Departamento de Microbiología, Facultad de Medicina, Universidad de Zaragoza IIS-Aragón, Zaragoza, Spain
[5]CIBER Enfermedades Respiratorias, Instituto de Salud Carlos III, Madrid, Spain
Co-senior authors
*Corresponding author. Center for Microbiology, VIB-KU Leuven, 3001 Leuven, Belgium
E-mail: jan.michiels@kuleuven.be

Abstract

Aims

We aimed to investigate the molecular mechanisms underlying the survival of *Mycobacterium abscessus* when faced with antibiotic combination therapy. By conducting evolution experiments and whole genome sequencing (WGS), we sought to identify genetic variants associated with stress response mechanisms, with a particular focus on drug survival and resistance.

Methods and results

We conducted evolution experiments on *M. abscessus*, exposing the bacteria to a combination therapy of amikacin and rifabutin. Genetic mutations associated with increased antibiotic survival and altered susceptibility were subsequently identified by WGS. We focused on mutations that contribute to stress response mechanisms and tolerance. Of particular interest was a novel frameshift mutation in *MAB_3509c*, a gene of unknown function within the upstream open reading frame of *whiB7*. A *MAB_3509c* knockout mutant was constructed, and expression of downstream drug resistance genes was assessed by RT-qPCR. Mutation of *MAB_3509c* results in increased RNA levels of *whiB7* and downstream stress response genes such as *eis2*, which is responsible for aminoglycoside resistance.

Conclusion

Our findings demonstrate the importance of *whiB7* in the adaptive stress response in *M. abscessus*. Moreover, our results highlight the complexity of *M. abscessus* adapting to drug stress and underscore the need for further research.

Impact statement

Interventional therapy options for *M. abscessus* infections are severely limited, and antimicrobial resistance further restricts available treatments, leading to prolonged, poorly tolerated regimens with suboptimal outcomes. Here, we investigate a polymorphism in the upstream open reading frame of *whiB7*, which contributes to increased resistance in *M. abscessus*. Understanding the mechanisms behind WhiB7 induction offers novel insights into intrinsic resistance and may serve as a valuable tool in drug discovery.

Keywords

Mycobacterium abscessus, amikacin, clarithromycin, *whiB7*, antimicrobial resistance, evolution experiments

Introduction

Bacterial infections rank among the foremost health threats in the 21st century (1). With an estimated 10.6 million infections and 1.3 million deaths in 2022, *Mycobacterium tuberculosis* is a bacterial pathogen of major importance, particularly in low-income countries, and global efforts to combat tuberculosis remain an absolute priority (2). At the same time, the incidence of non-tuberculous mycobacterial (NTM) infections is on the rise, especially in high-income countries (3).

Non-tuberculous mycobacteria comprise over 170 species, with *Mycobacterium avium* complex (MAC) and *Mycobacterium abscessus* complex (*M. abscessus*) emerging as significant causes of pulmonary disease (NTM-PD), particularly in vulnerable populations such as individuals with cystic fibrosis (CF) and other immunocompromising conditions (3, 4). While MAC infections account for most NTM-PD cases, *M. abscessus* infections, though less common (3-13% of NTM-PD cases), are far more challenging to treat (5). Notably, *M. abscessus* causes over 50% of NTM infections in CF patients, with a prevalence of 4.1% in this population (5, 6). Alarmingly, the global incidence of *M. abscessus* infections is rising as a result of improved detection and a genuine increase in infection rates (7).

Treatment options for *M. abscessus* NTM-PD are currently scarce due to the pathogen's inherent drug resilience. Efficient treatment is further impeded by our limited understanding of pathogenesis, difficulties in subspecies identification, and substantial variation in treatment response among the three subspecies *M. abscessus abscessus*, *M. abscessus bolletii* and *M. abscessus massiliense* (8–10). Empirical treatment schemes of choice typically comprise a combination of a macrolide, imipenem or cefoxitin, and an intravenously administered aminoglycoside such as amikacin (AMK). These regimens typically last several months, followed by an additional year of treatment post-sputum conversion, and are poorly tolerated. In addition, success rates are disappointingly low (estimated at below 50%), which can largely be attributed to the pathogen's resistance and tolerance mechanisms (8, 11–13).

M. abscessus exhibits a range of resistance mechanisms, encompassing both acquired resistance to aminoglycosides and fluoroquinolones, and intrinsic resistance mechanisms to most antibiotic classes. These resistance mechanisms are critical determinants of treatment success and pose significant challenges in clinical management (13–15). A well-documented example is macrolide resistance. Macrolides bind to 23S rRNA, thereby inhibiting bacterial protein synthesis (16). Acquired resistance to macrolides in *M. abscessus* is frequently associated with point mutations in the *rrl* gene, encoding 23S rRNA. The susceptibility of *M. abscessus* to macrolides, particularly azithromycin and clarithromycin (CLA), is crucial for treatment success. However, macrolide efficacy varies significantly among the three subspecies (10, 17). *M. abscessus abscessus* and *M. abscessus bolletii* exhibit reduced susceptibility to macrolides due to the presence of a functional erythromycin ribosome methyltransferase gene *erm(41)*, whose gene product methylates 23S rRNA (17, 18). Low-level exposure to macrolides induces the mycobacterial transcriptional regulator WhiB7, which in turn activates *erm(41)* expression. Over time, drug-sensitive *M. abscessus abscessu*s and *M. abscessus bolletii* strains can therefore develop high-level resistance if exposed to macrolides. Conversely, *M. abscessus massiliense* lacks a functional *erm(41)* gene, thereby maintaining prolonged sensitivity to these antibiotics (18).

Resistance to rifamycins also relies on well-known genetic determinants. These antibiotics inhibit bacterial transcription by binding to the *rpoB*-encoded β-subunit (RpoB) of the DNA-dependent RNA polymerase, and they form a cornerstone drug in the treatment of tuberculosis (19). However, rifamycins are rendered ineffective against *M. abscessus* by drug-modifying enzymes, oxidation enzymes (*rox*), and ribosylation enzymes (*arr*) (20). To address these limitations, modified rifamycins such as rifabutin (RFB) and rifaximin, are currently being explored (13, 21).
Among the most effective antibiotics against *M. abscessus* are aminoglycosides of which AMK is a prime example. The latter exerts its antibacterial effects by binding to the 16S rRNA of the 30S ribosomal subunit, leading to the mistranslation of proteins. AMK is typically administered intravenously but inhaled formulations are also being explored (8, 22). Despite its potency, AMK's severe adverse effects, including ototoxicity, nephrotoxicity, and tinnitus pose significant challenges to its therapeutical use (22, 23). Furthermore, various mutations in the 16S RNA binding site are known to confer resistance to high levels of AMK. Additionally, the susceptibility of *M. abscessus* to AMK is affected by WhiB7 as it activates expression of *eis2* and *aac(2')* encoding acetyltransferase enzymes that inactivate AMK (23).

Drug resistance is not the sole factor contributing to antibiotic survival as other survival mechanisms including tolerance and persistence also play a critical role in treatment failure. These mechanisms have been extensively studied in rapidly proliferating bacteria (24–26), and are now also a research topic of interest in mycobacteria. *M. tuberculosis* has been demonstrated to form small subpopulations of persister cells that display transient multidrug tolerance while being genetically identical to their susceptible kin (27). These persister cells typically exhibit reduced metabolic activity and low ATP levels. Various stressors are known to deplete energy resources, thereby fostering drug tolerance. In addition, impairing the biosynthesis of phthiocerol dimycocerosate (PDIM) has been shown to increase persister levels (28). Conversely, enhanced cellular respiration has been demonstrated to mitigate such tolerance (29). Current persistence research focuses on elucidating the roles of several key biological processes involved in asymmetric cell division, toxin-antitoxin systems, biofilms, sigma factors, and the mycobacterial stringent response in drug tolerance and survival (30). Despite *M. abscessus*'s unique susceptibility and genetic profile, current persistence research only revolves around *M. tuberculosis*.

M. abscessus activates tailored responses to antibiotics, including drug-specific tolerance mechanisms like enzyme conversion, target protection, and metabolic shifts, though further validation is needed (15). Survival mechanisms often involve transcriptional regulators controlling genes with largely unknown functions in stress responses, leading to multidrug resistance (15, 31–33). For instance, VapC5 induces a growth-arrested state, enhancing persister formation and drug survival by inactivating $tRNASer^{CGA}$, thereby reprogramming its transcriptome to favor *whiB7* expression and facilitating drug survival against AMK and other ribosome-targeting antibiotics (34). These findings highlight the importance of physiological adaptation in drug survival, with the mycobacterial transcriptional regulator WhiB7 playing a seemingly pivotal role. Nonetheless, our understanding of the molecular mechanisms underpinning antibiotic survival in *M. abscessus* remains incomplete and fragmented. The current and future treatment regimens for *M. abscessus* continue to rely on combinations of antibiotics from different classes. This multi-drug approach is crucial for preventing drug resistance (35, 36). However, antibiotics within the regimen can provoke a stress response that impacts the efficacy of other antibiotics and despite combinational approaches, *M. abscessus* can accumulate mutations that confer tolerance and resistance. To elucidate the mutations responsible for drug survival in a multi-drug context, we conducted an experimental evolution study, selecting for surviving populations.

Our results led us to identify a novel frameshift mutation in *MAB_3509c*, located within the upstream open reading frame (*uORF*) of *whiB7*. This mutation confers significant resistance to AMK and alters CLA susceptibility by markedly increasing RNA levels of *whiB7* and its downstream stress response genes, including *eis2*, which is implicated in aminoglycoside resistance. These findings underscore the pivotal role of *whiB7* induction in conferring multidrug resistance in *M. abscessus* and illustrate the intricate mechanisms by which this pathogen adapts to antibiotic stress. Further investigation into these regulatory pathways is essential for developing more effective treatment strategies and improving clinical outcomes for patients suffering from these challenging infections.

Materials and methods

Bacterial strains and growth conditions

M. abscessus ATCC19977 strains were cultivated at 37 °C while shaking at 110 rpm in Middlebrook 7H9 (BD 271310) supplemented with 0.05% (vol/vol) Tween 80 (Sigma, P4780) and enriched with 10% (vol/vol) OADC (BD 211886). Bacterial cultures were plated on Middelbrook 7H10 (BD 262710) agar plates supplemented with 0.05% (vol/vol) Tween 80 (Sigma, P4780), 0.5% (vol/vol) glycerol (Difco, 228220) and enriched with 10% (vol/vol) OADC (BD 211886) and incubated at 37 °C.

Construction of a *MAB_3509c* knockout (*ΔuORF*)

The *MAB_3509c* gene, located upstream of *MAB_3508c* (*whiB7*), was replaced by a Zeocin resistance cassette via recombineering as described previously (37). Briefly, *M. abscessus* expressing recombineering proteins from the pJV53 plasmid was electroporated with 500 ng allelic exchange substrate (AES), synthetized by GenScript. The AES was designed to preserve 48 bp and 41 bp at the beginning and end of the gene, respectively, and contains 1000 bp homologues arms up-and downstream of the targeted region, with a Zeocin resistance cassette inserted between the flanking regions (**Table S1**). Transformants were selected on agar plates containing 50 µg/mL Zeocin (Gibco, R25001). Recombinant clones were picked after 1 week of incubation at 37 °C and confirmed using PCR amplification followed by Sanger sequencing. Primer sequences are provided in **Table S2**.

Evolution under drug combination pressure

A clear streak of *M. abscessus* was made, from which three ancestral colonies were picked and cultivated to an OD600 > 1. For each ancestor, the resulting culture was split over four flasks, three of which were parallelly treated with a combination of 100 µg/mL AMK (Sigma, A3650) and 10 µg/mL RFB (Sigma, R3501) and incubated statically at 37 °C. The fourth flask was treated with DMSO as a control. Bacterial populations were enumerated at days 0, 3, 5, 7, 10, and 14 through serial dilution in PBS and plating on agar plates, followed by incubation for 7 days at 37 °C. On day 7, 2 mL samples were spun down and washed three times with PBS. The resulting pellet was resuspended in 10 mL fresh antibiotic-free medium, and samples were again incubated. Following growth, cultures were diluted based on their OD600 values, using a calculated dilution factor that assumed a 3-hour doubling time to ensure they reached an OD600 of 1 the following day. Glycerol stocks were prepared from regrown cultures and stored at -80 °C. The remaining culture was used for enumeration and the construction of killing curves.

Antimicrobial susceptibility testing

Cultures were assessed for the emergence of drug resistance using a resazurin microtiter assay (REMA) (38). The protocol was modified to allow the detection of low-frequency resistance in bacterial populations. In summary, cultures were grown to mid-log exponential phase and normalized to an OD600 of 0.4. Samples were diluted 300× in culture medium, and 200 µL was added to a 96-well microtiter plate containing serial 2-fold dilutions of antibiotics. The latter was prepared by transferring 0.5 µL of antibiotic solution to a 96-well microtiter plate using an Echo acoustic liquid handler. Bacteria were incubated in the presence of antibiotics for 72 hours at 37 °C, followed by the addition of 30 µL resazurin (0.1 mg/mL). After an additional 24-hour incubation, wells that remained blue were deemed negative for growth, while a color shift to pink was considered indicative for growth. Minimum inhibitory concentrations (MIC) were defined as the average concentration at which no color change was observed, *i.e.*, it was visually indistinguishable from the “no bacteria”

control. MIC values were compared relative to a reference strain, which was included in each susceptibility assay.

Whole genome sequencing (WGS)

Genomic DNA from selected clonal survivors was extracted using the ZR Fungal/Bacterial DNA Miniprep kit (Zymo Research) following the manufacturer's protocols. WGS libraries were prepared using the Nextera XT DNA Library Preparation Kit (Illumina). Sequencing was performed on an Illumina NextSeq 550 platform, generating paired-end 75 bp reads. The trimmed reads were mapped to the reference genome of *M. abscessus* ATCC 19977 (GenBank accession number CU458896.1), and variants were identified using the CLC Genomics Workbench v21.0.5 (Qiagen) variant caller, with a minimum coverage of 10 and a minimum frequency of 10%. To detect low-frequency variants in mixed populations within the rifampicin resistance-determining region (RRDR) of *rpoB*, variants were identified at the read level, with manual filtering to exclude misalignments and sequencing artifacts.

Selection of clones surviving antibiotic treatment

Undiluted, 10× diluted and 1000× diluted mixed populations obtained after rounds 3 and 4 of combination drug pressure were challenged on agar plates containing RFB at 32× and 128x the MIC (26.5 and 160 µg/mL, respectively). After 7 days of incubation at 37 °C, colonies were picked and regrown in antibiotic-free medium. A total of 59 colonies were screened for the presence of *rpoB* mutations in the rifampicin resistance-determining region (RRDR) using PCR amplification and Sanger sequencing (see **Table S2** for primers). Clones with RRDR mutations (34 in total) were excluded from further analysis. Six independent clones lacking RRDR mutations were subjected to MIC characterization.

Quantitative PCR

A previously described reverse transcription-quantitative PCR (RT-qPCR) protocol (38) was adapted to quantify expression of *whiB7* and its downstream regulated resistance genes – *eis2*, *erm(41)*, and *aac(2')* – in the *uORF** mutant and the Δ*uORF* knockout. Expression levels were compared to those of relevant control strains in the absence and presence of CLA, which has been demonstrated to be a potent inducer of *whiB7* expression in wild-type *M. abscessus* strains (39). The different *M. abscessus* strains were cultured to an OD600 of 0.3 to 0.5 in culture medium. Cultures were divided into six 10 mL aliquots and treated with 2 µg/mL CLA or an equal volume of DMSO for control samples, resulting in biological triplicate samples per condition. After 3 hours of shaking incubation at 37 °C, 20 mL of RNAprotect Bacteria Reagent (Qiagen, 76506) was added to each tube containing 10 mL of bacterial culture. The mixture was vortexed for 5 seconds, incubated for 10 minutes at room temperature, and pelleted at 5000 g for 10 minutes.

Total RNA was extracted using the ZYMO bacterial and fungal RNA isolation kit, including an in-column DNase I (Qiagen 79254) treatment. RNA was further treated with dsDNAse (Thermo Fisher EN0771) according to the manufacturer's protocol. RNA quality was assessed using a Nanodrop 1000 and an Agilent TapeStation RNA kit. Approximately 100 ng of total RNA was used as input for cDNA synthesis with the Maxima H Minus First Strand cDNA Synthesis Kit protocol using random primers. The cDNA was diluted 10×, and 2.5 µl of the diluted cDNA was used in each 25 µl quantitative PCR reaction, following the Applied Biosystems™ SYBR™ Green Universal Master Mix protocol. Primer sequences for each gene target are listed in **Table S2**.

Reactions were run on a LightCycler 480 detection system with cycling conditions: 50 °C for 2 min, 95 °C for 10 min, and 40 cycles of 95 °C for 15 s and 60 °C for 1 min. Ct values were normalized to the

Ct value of the housekeeping gene *sigA*, amplified from the same cDNA sample. Changes in expression between conditions were calculated using the $2^{-\Delta\Delta Ct}$ method. GraphPad Prism (v10.2.2) was used to construct graphs, with error bars representing the standard deviation from biological triplicates. Ct differences between conditions were assessed using a 2-way ANOVA test.

Detection and structure prediction of elements upstream of *whiB7*

Elements upstream of the *whiB7* gene were predicted through similarity to published nucleotide sequences in other mycobacteria (40). Predicted structural elements were confirmed using the RNA structure prediction tool RNAFold, part of the ViennaRNA web services (41).

Extraction of *whiB7* gene sequences from a clinical isolate *in silico* library

The upstream *whiB7* sequences, including *MAB_3509c* and possible regulatory elements, were extracted through a proprietary BLAST-based search tool targeting 97% minimum identity and 90% minimum coverage of reference sequences from *M. abscessus* ATCC 19977 (GenBank accession number CU458896.1). These parameters ensured the accurate extraction of the region from all strains in our collection, without generating false positives. The resulting FASTA files were mapped against the *M. abscessus* ATCC19977 (subspecies *abscessus*) reference genome to identify variants.

Results

Increased survival of *M. abscessus* after successive treatment rounds with AMK and RFB

Our primary objective was to elucidate the mechanisms that facilitate drug survival in *M. abscessus abscessus* and to assess a potential role in the emergence of drug resistance. To this end, an evolution experiment was conducted to unravel genetic mutations that contribute to increased multi-drug survival (**Figure 1A**). Nine cultures of *M. abscessus* were grown to stationary phase and subsequently exposed to a combination of an aminoglycoside (AMK) and a rifampicin analogue (RFB). Antibiotic concentrations well above the MIC were used to ensure effective bacterial killing and to minimize the risk of resistance development. It is noteworthy that treatment with a single antibiotic led to the emergence of resistance within the initial treatment cycle, which was not observed in the combination treatment (**Figure S1**). After 7 days of drug exposure, a portion of the bacterial population was washed and regrown in an antibiotic-free medium before repeating the antibiotic challenge. The remaining culture was enumerated to assess bacterial survival and to construct killing curves (**Figure 1B**). The procedure was repeated over a total of four rounds. By the end of the fourth cycle, the mean bacterial survival rate at day 7 had increased from 0.02% to 0.51% (**Table S3**).

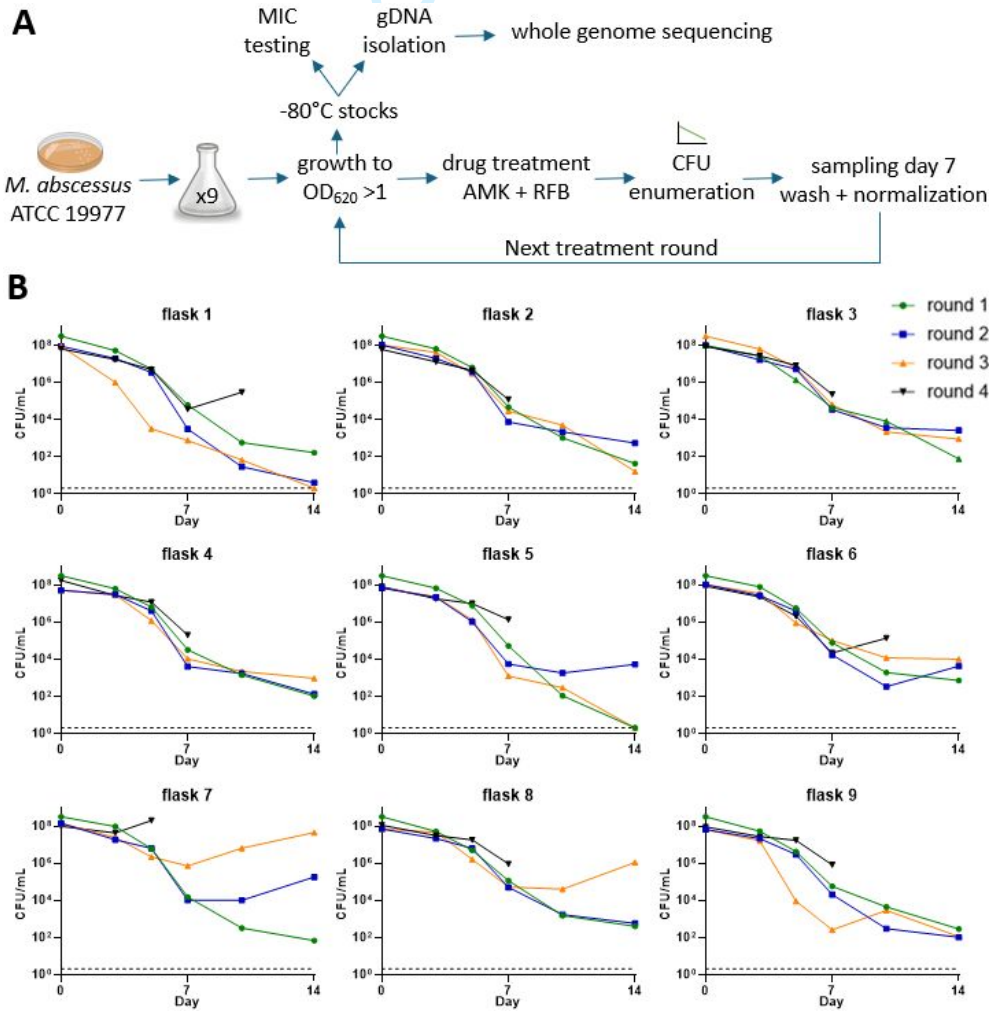

Figure 1. **Experimental evolution of *M. abscessus* under combined AMK and RFB pressure. (A)** Experimental design: Bacterial cultures were grown to an OD600 > 1 and subsequently exposed to a combination of AMK (100 µg/mL, 25× MIC) and RFB (10 µg/mL, 12× MIC) drug pressure for a period of 14 days. After 7 days, a portion of the population was washed and regrown in antibiotic-free medium before repeating the antibiotic challenge. The remaining culture was enumerated to construct killing curves. Regrown cultures underwent MIC testing, and selected mixed populations were subjected to WGS.

(B) Time-kill curves for each treatment round with AMK and RFB combination for nine flasks. Round 1 (□, green), round 2 (■, blue), round 3 (▲, orange), round 4 (▼, black).

To monitor the development of decreased sensitivity, the MIC of the individual antibiotics was assessed in mixed populations that were re-grown after 7 days of drug exposure (**Error! Reference source not found.**). The study was concluded after four rounds of antibiotic challenges, at which point high-level AMK resistance (> 64 µg/mL) had emerged in all flasks. Notably, reduced RFB susceptibility typically manifested one round after the emergence of AMK resistance.

Table 1. MIC fold changes of populations relative to the wild-type ancestor strain. Susceptibility testing was performed with regrown survivors of day 7 using a broth resazurin assay. Fold increases in MIC relative to the ancestral strain are shown, with changes of 4x and above in bold. Antibiotics tested: amikacin (AMK) and rifabutin (RFB). The MIC for 1x AMK corresponds to 4 µg/mL, and 1x RFB corresponds to 0.85 µg/mL. Clarithromycin and moxifloxacin were used as controls and the MIC of both antibiotics remains unaltered (data not shown).

	Flask 1	Flask 2	Flask 3	Flask 4	Flask 5	Flask 6	Flask 7	Flask 8	Flask 9	
AMK	2x	2x	1x	1x	1x	1x	1x	1x	2x	Round 1
RFB	2x	1x	1x	1x	1x	1x	1x	1x	1x	
AMK	2x	2x	1x	**4x**	2x	1x	**> 16x**	1x	2x	Round 2
RFB	1x	1x	1x	1x	1x	1x	1x	1x	1x	
AMK	2x	**> 16x**	**> 16x**	**> 16x**	**16x**	**> 16x**	**> 16x**	**> 16x**	**> 16x**	Round 3
RFB	1x	1x	1x	1x	1x	1x	**8x**	**4x**	1x	
AMK	**> 16x**	**> 16x**	**> 16x**	**> 16x**	**> 16x**	**> 16x**	**> 16x**	**> 16x**	**> 16x**	Round 4
RFB	1x	1x	**8x**	1x	**> 16x**	**8x**	**> 16x**	**> 16x**	**16x**	

Mutations in the 16S *rrs* gene confer resistance to AMK, while *rpoB* mutations can only partly explain reduced RFB susceptibility

To identify the genetic mutations responsible for the emergence of resistance, WGS was performed on populations exhibiting resistance. The sequencing reads were aligned against the *M. abscessus* ATCC19977 reference genome. Following the filtering of variations observed in the *M. abscessus* strain used in this work relative to the reference genome, some additional polymorphisms were identified in the ancestral clones used to initiate the evolution experiment. Specifically, the ancestor used to inoculate flasks 4, 5, and 6 harbored three single nucleotide variants (SNVs) in *MAB_1020*, *MAB_3454c*, and *MAB_4311c*. The ancestor selected for flasks 7, 8, and 9 exhibited a SNV in *MAB_2285*. Susceptibility testing demonstrated that there were no notable differences in the susceptibility profiles of the ancestral strains (data not shown). Consequently, these ancestral SNVs were excluded from downstream analysis.

WGS identified several SNVs and insertion-deletion mutations (indels). Notably, no recurrent mutations were found in the nine evolved populations, except for mutations in two genes previously documented to be involved in resistance, *rrs* (*MAB_r5051*) and *rpoB* (*MAB_3869c*). Following four rounds of evolution, a dominant A1408G substitution (*E. coli* numbering (42)) in *rrs* (*MAB_r5051*) was identified in all nine populations. The *rrs* gene encodes 16S rRNA and the identified mutation has previously been reported to cause high-level resistance to 2-deoxystreptamine aminoglycosides,

including AMK, in *M. abscessus* (23). It is therefore likely that this mutation is responsible for the observed AMK resistance in our evolved populations.

As evidenced from **Error! Reference source not found.**, a decrease in sensitivity to RFB emerged in six out of nine lines after four rounds of evolution. Rifamycin resistance has previously been associated with mutations in *rpoB* (*MAB_3869c*) encoding the β subunit of RNA polymerase (43). However, WGS showed that an *rpoB* mutation only occurred in one population (flask 7). This C1355T mutation (*M. abscessus* ATCC19977 numbering) results in an S452L substitution in the mycobacterial rifampicin resistance-determining region (RRDR) of *rpoB*, and has previously been associated with RFB resistance in *M. abscessus* (43). Upon revisiting the sequencing data from the same populations, a more detailed read-level analysis revealed a low frequency of C1355T (S452L) *rpoB* mutations in three additional populations: 5.8% in flask 5, 5.7% in flask 8, and 3.6% in flask 9. Additionally, an *rpoB* C1355G (S452W) mutation was found in 2.9% of the reads in flask 5. Finally, an *rpoB* A1301T (Q434L) mutation was identified in flask 8 and flask 9, with a frequency of 7.3% and 1.1% of the reads, respectively. These mutations were present in cultures with increased RFB MICs. However, for two out of six cultures (flask 3 and 6), the observed 8-fold reduction in RFB susceptibility could not be attributed to *rpoB* mutations in the RRDR.

A *uORF whiB7* frameshift mutation is responsible for AMK and CLA survival

Since the identified mutations did not fully account for the observed susceptibility phenotypes, cells from evolved populations obtained at round 3 and round 4 were inoculated on high-concentration RFB plates at 32× MIC (26.5 µg/mL) to further investigate resistance. A total of 59 colonies were isolated and subjected to Sanger sequencing to identify mutations in the RRDR of *rpoB*. Mutations C1355T (S452L), C1355G (S452W) and A1301T (Q434L), which we previously observed at the population level, were confirmed in clones from flask 3, 4, 5, 7, 8 and 9. Additionally, a C1339T (H447Y) RRDR mutation was identified in round 4, flask 4 clones. Six independent clones lacking RRDR mutations were subjected to MIC determination (**Table 2**).

Table 2. MIC values of AMK and RFB of individual clones isolated after rounds 3 or 4 of the evolution experiment. The nomenclature refers to flask F (1, 4, 5 or 6), round R (3 or 4) and clone (a or b). Fold increases in MIC relative to the ancestral strain are shown. Antibiotics tested: amikacin (AMK) and rifabutin (RFB). Fold increases that exceed the upper concentration limit of the assay are indicated with a ">" symbol and presented in bold.

	F1R4a	**F4R3a**	**F5R3a**	**F6R3a**	**F6R4a**	**F6R4b**
AMK	2.67x	2.67x	**> 2.67x**	1.33x	**> 2.67x**	**> 2.67x**
RFB	1,5x	1.5x	1x	2x	**> 32x**	**> 32x**

Unexpectedly, four out of six clones did not have an increased MIC for RFB in broth, despite being recovered from the antibiotic agar plate. This discrepancy may be attributed to a number of factors, including potential degradation and diffusion of drugs, inoculation size effects, or phenotypic variation (25, 44, 45). Nevertheless, it is plausible that the isolated bacteria still possess causal mutations that allow them to initially survive and subsequently grow when drug concentrations are reduced. To elucidate the genotype-phenotype associations, clones exhibiting both increased and non-increased MIC values were subjected to variant detection analysis through WGS (**Table 3**).

Table 3. Genetic variants present in individual clones isolated after round 3 or round 4 of the evolution experiment. See **Table 2** for nomenclature.

Gene	Gene function	genetic change; protein change	F1R4a	F4R3a	F5R3a	F6R3a	F6R4a	F6R4b
MAB_r5051, rrs	16S ribosomal RNA	A1408G; na					x	x
MAB_3595c	Adenosylhomocysteinase	A1220G; H407R						x
MAB_r5052, rrl	23S ribosomal RNA	C2847A; na	x					
MAB_r5052, rrl	23S ribosomal RNA	C2655T; na		x				
MAB_3509c	Hypothetical protein	133delG; frameshift			x			

Curiously, while F6R3a exhibits minor shifts for AMK and RFB susceptibility, it does not harbor any discernible genetic mutations. Conversely, WGS analysis could (partially) explain the susceptibility phenotypes of some clones. For instance, F6R4a and F6R4b exhibit reduced AMK susceptibility due to the previously described A1408G substitution in *rrs* (*MAB_r5051*). However, while both clones are resistant to RFB, only F6R4b contains an additional mutation. The latter causes a non-synonymous A1220G substitution in *MAB_3595c* encoding adenosylhomocysteinase, which has not previously been linked with drug resistance.

Low level AMK resistance was observed for F1R4a and F4R3a. Both clones acquired mutations (C2847A and C2655T, respectively) in *rrl* (*MAB_r5052*) encoding 23S ribosomal RNA. Mutations in *rrl* have previously been associated with resistance in *M. abscessus* to multiple antibiotics, including linezolid and CLA. However, there is currently no evidence to suggest that these mutations contribute to AMK resistance (46, 47). Likewise, 23S mutations are known to confer resistance to other aminoglycosides (capreomycin and viomycin) in *M. tuberculosis*, but not to kanamycin or AMK (48).

Clone F5R3a exhibits AMK resistance and harbors a 133delG mutation in *MAB_3509c*. Interestingly, there is no annotated predicted gene function for *MAB_3509c*, and BLAST searches for both nucleotide and protein sequences yielded no hits in other mycobacterial species, except for those closely related to *M. abscessus*. The 133delG frameshift mutation leads to a truncated predicted protein which is terminated prematurely by a stop codon (**Figure 2A**). *MAB_3509c* is located 169 bp upstream of *MAB_3508c* as illustrated in **Figure 2B**. The latter shows 75% identity to *Mycobacterium smegmatis* and *M. tuberculosis whiB7*, encoding a conserved mycobacterial transcriptional activator that promotes various drug resistance determinants (49). In *M. abscessus*, WhiB7 has been shown to elicit a species-specific response (39), being induced by different ribosome-targeting antibiotics, including AMK and CLA. Deletion of *whiB7* prolongs susceptibility to erythromycin, CLA, spectinomycin, AMK, and tetracycline by blocking the inducible stress response (39).

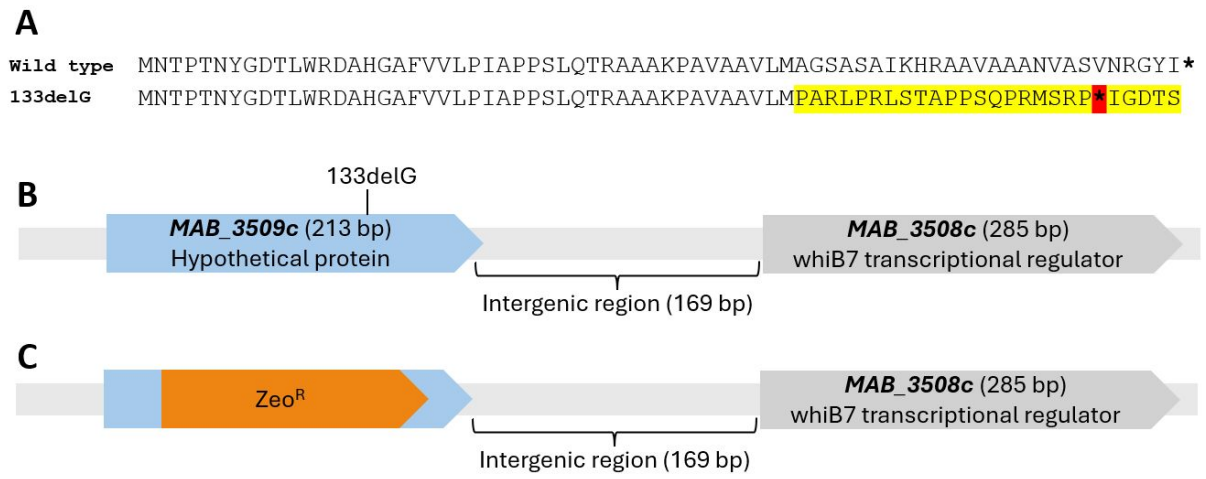

Figure 2. *M. abscessus MAB_3509c* sequence and genomic region. (A) Comparative protein alignment of the translated wild-type *MAB_3509c* gene and the 133delG *MAB_3509c* mutant, highlighting changes in amino acids (marked in yellow) resulting in the formation of a premature stop codon (red). **(B)** Genomic representation of the *MAB_3509c* gene, upstream of *MAB_3508c*, a homolog of the conserved mycobacterial regulator *whiB7*. For clarity, the orientation of *MAB_3508c* and *MAB_3509c*, which are situated on the minus strand of the *M. abscessus* ATCC19977 reference genome, is reversed in this depiction. **(C)** Schematic representation of the *ΔuORF* construct, with the *MAB_3509c* gene replaced by a Zeocin resistance cassette.

In *Actinobacteria*, it has been show that *whiB7* genes are frequently preceded by a *uORF* which regulates *whiB7* expression through attenuation mechanisms (40, 50). We hypothesized that the identified 133delG mutation in *MAB_3509c*, hereafter referred to as '*uORF**', confers resistance to AMK and CLA by activating the WhiB7 stress response, possibly by disruption of ORF-mediated transcription attenuation, as observed in other mycobacteria (51). To investigate the role of the *uORF* in the WhiB7 stress response, we generated a *MAB_3509c* knockout via recombineering, incorporating a Zeocin resistance cassette to replace *MAB_3509c* (**Figure 2C**). This knockout strain is referred to as '*ΔuORF*'.

Since WhiB7 is responsible for multidrug resistance, these mutants were subjected to MIC testing, including other anti-*M. abscessus* drugs (**Table 4**). Following a 4-day incubation period, the *uORF** mutant exhibited a 5.3-fold increase in MIC for AMK and a 4-fold increase for CLA, whereas the Δ*uORF* mutant demonstrated increased susceptibility to both AMK and CLA. The MIC for moxifloxacin (MOX), RFB and bedaquiline (BDQ) remained unaffected by either mutation. After an extended incubation period of 14 days at 37°C, induced resistance to CLA was observed in both the ancestor wild-type strain and the *uORF** mutant, with the MIC reaching the upper limit of the MIC assay at 32 µg/mL. In contrast, the Δ*uORF* mutant remained sensitive at 6 µg/mL (data not shown). These findings suggest that the *uORF** mutation triggers a WhiB7-like stress response, conferring resistance to both AMK and CLA, while the knockout of the upstream region leads to sensitivity by preventing *whiB7* induction.

Table 4. **MIC fold changes for *uORF** and *ΔuORF* relative to reference strains after a 4-day incubation period.** *M. abscessus* ATCC19977 was used as the reference for the Δ*uORF* knockout. For the *uORF** mutant, the ancestral clone used to initiate the evolution experiment was included as a control. Antibiotics tested: amikacin (AMK), bedaquiline (BDQ), clarithromycin (CLA), moxifloxacin (MOX), rifabutin (RFB).

	*uORF**	*ΔuORF*
AMK	5.3x	0.5x
BDQ	0.67x	1x
CLA	4x	0.125x
MOX	1x	1x
RFB	1x	1.25x

The *uORF causes elevated expression of *whiB7* and downstream drug resistance determinants**

Across the genus Mycobacterium, the WhiB7 stress response is known to be triggered by environmental stressors and ribosome-targeting antibiotics, such as macrolides and aminoglycosides, which activate resistance genes in the WhiB7 regulon (39, 52). We hypothesized that the observed AMK and CLA resistance in the uORF* mutant (**Table 4**) could be attributed to induction of the WhiB7 stress response. To investigate this, we performed RT-qPCR to quantify the expression levels of downstream regulated resistance genes – eis2, erm(41), and aac(2') – in both the uORF* mutant and the ΔuORF knockout. To ensure that the effects observed were attributed to the uORF mutations, we included as controls both the ancestor of flask 5, from which the uORF* was selected, and our wild-type M. abscessus ATCC 19977 stock strain, from which ΔuORF was derived. Expression levels were measured in both the absence and presence of CLA, which is known to strongly induce whiB7 expression in wild-type strains (39).

To evaluate the inducibility of the WhiB7 stress response under CLA pressure in both mutant and control strains, we compared induction levels in the presence of CLA relative to a DMSO control (**Error! Reference source not found.A)**. Notably, *whiB7* expression in the *uORF** and *ΔuORF* mutants exhibits limited induction (~11-fold) in response to CLA. In contrast, *whiB7* levels in control strains with an intact upstream region (ancestor and wild type) increase more than 200-fold. This is in line with an earlier report showing elevated *whiB7* expression and increased levels of *eis2*, *erm(41)*, and *aac(2')* in response to CLA (38).

In the absence of CLA (DMSO control), RNA levels for all tested genes are comparable in the control strains (ancestor and wild type) (**Error! Reference source not found.B**). However, in these conditions, the *uORF** mutant displays markedly elevated *whiB7* levels (10-fold), with *eis2* increasing 28-fold, and *erm(41)* and *aac(2')* increasing more than 3-fold compared to the ancestor. Therefore, the reduced inducibility of the *uORF** mutant (**Error! Reference source not found.A**) can be attributed to its elevated RNA levels under non-stressed conditions. Furthermore, these elevated expression levels under non-stressed conditions likely contribute to *M. abscessus*-specific AMK resistance (39). In contrast, the *ΔuORF* mutant shows expression levels similar to the wild-type strain under non-stressed conditions (**Error! Reference source not found.B**), which is in line with the data shown in **Table 4**.

Upon CLA treatment, expression levels of tested genes are not significantly different in both control strains (ancestor and wild type) (**Error! Reference source not found.C**). Likewise, the expression differences between the *uORF** mutant and its ancestor disappear, with both strains exhibiting

comparable expression levels of *whiB7* and its downstream genes. However, the *ΔuORF* mutant fails to induce a robust WhiB7 stress response, as evidenced by significantly lower expression levels of *whiB7*, *eis2*, *erm(41)*, and *aac(2')* compared to the wild type. This lack of inducibility is likely due to the loss of the *uORF* regulatory mechanism that typically facilitates induction in response to CLA.

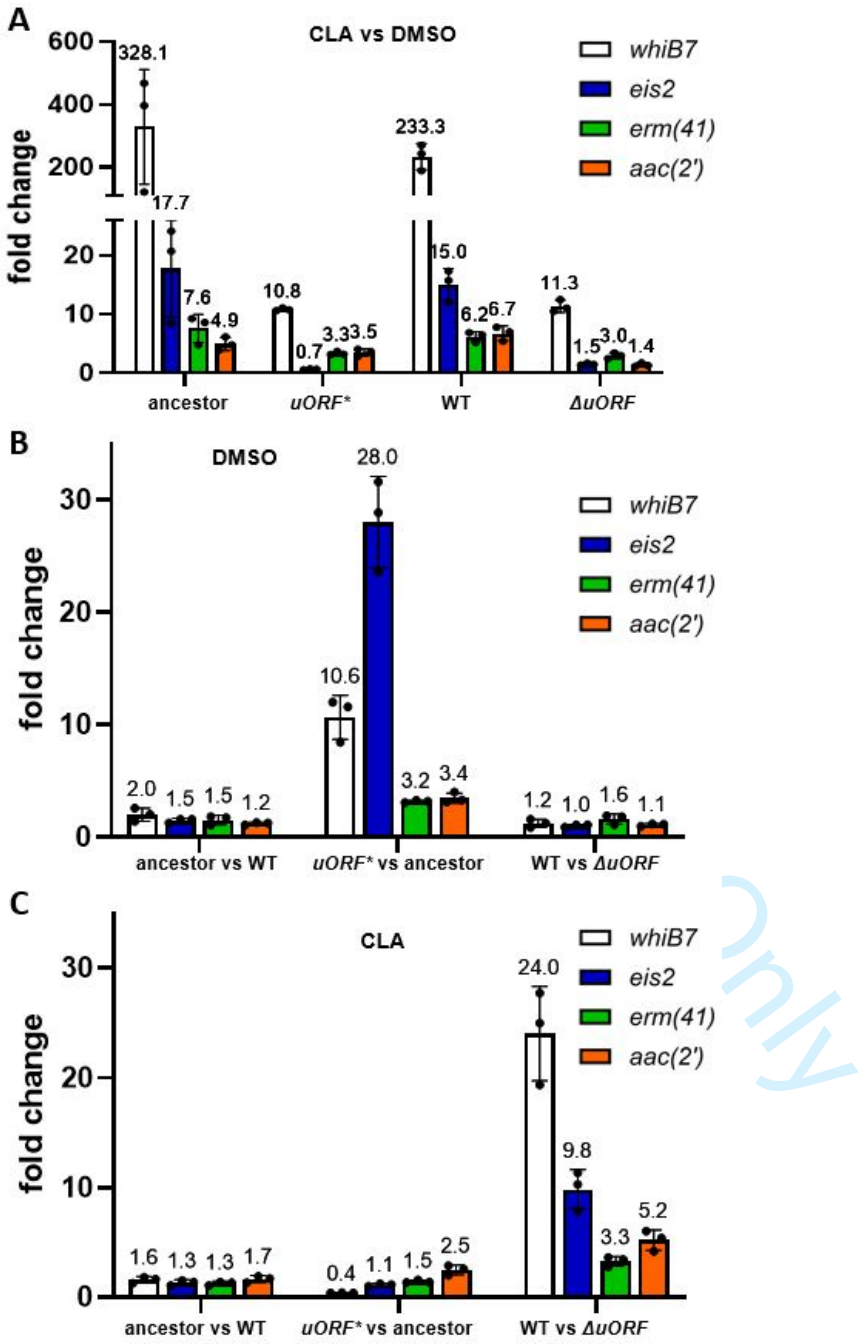

Figure 3. Transcription levels of *whiB7*, *eis2*, *aac(2')*, and *erm(41)* quantified by RT-qPCR. Expression was assessed in the ancestral clone of the evolution experiment (ancestor), the evolved clone with a 133delG mutation in *MAB_3509c* (*uORF**), the *M. abscessus* ATCC19977 wild type (WT) and its derived *MAB_3509c::Zeo*^{R} knockout (*ΔuORF*). Cultures were grown to exponential phase and treated for 3 hours at 37 °C with either 2 µg/mL CLA or DMSO (control). Expression levels are shown relative to those of the housekeeping gene *sigA*. Data are the mean of three biological repeats, with error bars representing standard deviation. **(A)** Fold change expression after 3 hours exposure to 2 µg/mL CLA relative to the DMSO control expression levels. **(B)** Fold change comparison of gene expression levels in the absence of antibiotics (DMSO control): in the two control strains, ancestor and WT, in the *uORF** mutant compared to its ancestor, and in the wild type compared to the Δ*uORF* knockout mutant. **(C)** Fold change comparison of gene expression levels after 3 hours exposure to 2 µg/mL CLA: in the two control strains, ancestor and WT, in the *uORF** mutant compared to its ancestor, and in the wild type compared to the Δ*uORF* knockout mutant.

In summary, our results suggest that the *uORF** mutation causes constitutive activation of the WhiB7 stress response, even in the absence of stress inducers. We hypothesize that the observed *uORF** mutation disrupts a *uORF*-dependent transcriptional attenuation mechanism of the WhiB7 stress response by destabilizing an RNA terminator structure (see below). This destabilization likely results in increased *whiB7* expression and elevated antibiotic resistance, even in the absence of a stressor.

M. abscessus clinical isolates show DNA polymorphisms in the _uORF_ of _whiB7_

To gauge the prevalence of *uORF* mutations, a total of 222 *M. abscessus* genomes obtained from a set of clinical isolates were screened for genetic variants in the region proximal to *whiB7*. The set is comprised of 77, 120 and 2 genomes of the subspecies *M. abscessus abscessus*, *M. abscessus massiliense*, and *M. abscessus bolletii*, respectively. The remaining 23 genomes remain unclassified. The upstream *whiB7* sequences, including *MAB_3509c* and potential regulatory regions, were extracted and mapped against the *M. abscessus* ATCC19977 reference genome.

Notably, the specific guanine deletion mutation 133delG at base position –251, relative to the *whiB7* start codon, was not identified in any of the isolates. Moreover, no insertions or deletions were identified within the *MAB_3509c* region. However, 9 *M. abscessus abscessus* genomes harbored two SNVs at positions –420 (A>G) and–160 (A>G) that were conserved across these 9 strains. Two other *M. abscessus abscessus* strains harbored a SNV at position –487 (G>A). Additionally, all *M. abscessus massiliense* isolates exhibited two SNVs (C>G) in the *MAB_3509c* region at positions –260 and –286 and an adenine insertion at position –425, upstream of MAB_3509c, indicating conserved variations across subspecies. Interestingly, one subsp. *abscessus* isolate harbored a single G>A SNV at position –260, which is analogous to the variant observed in subsp. *massiliense*. These variations could impact the expression and function of the *whiB7* gene, contributing to varying levels of antibiotic resistance or hypersensitivity, as suggested for *M. tuberculosis* isolates (51, 53, 54). Further investigation into the precise effects of these mutations on *whiB7* expression in *M. abscessus* and the associated stress response is required to shed light on their role in drug resistance mechanisms.

Discussion

A *uORF* 133G deletion results in AMK and CLA resistance through constitutive *whiB7* expression

Our study has uncovered a novel frameshift mutation in the *MAB_3509c* gene, located within the *uORF* of *whiB7.* The *uORF** mutant harbors a guanine deletion at position –251 relative to the *whiB7* start codon and was serendipitously recovered from RFB plates following prolonged exposure to AMK and RFB combination pressure. This mutation results in enhanced resistance to both AMK and CLA. Given that susceptibility to both antibiotics is affected by the WhiB7 stress response, we examined *whiB7* expression under non-stressed conditions and CLA drug pressure to gain a deeper understanding of the underlying mechanisms.

Basal expression analysis revealed that, under non-stressed conditions, RNA levels for *whiB7, eis2, erm(41)*, and *aac(2')* are markedly higher in the *uORF** mutant compared to its ancestor strain. These elevated expression levels directly contribute to *M. abscessus*-specific resistance mechanisms for AMK and CLA through induction of the *eis2* and *erm(41)* genes by *whiB7* (18, 39). Following CLA treatment, the differences in expression are no longer evident, with the *uORF** and its ancestor exhibiting comparable expression levels, which suggests that the mutation mimics the antibiotic-induced activation mechanism of the WhiB7 stress response. Moreover, the *ΔuORF* mutant, which lacks *MAB_3509c* but retains the intergenic sequence, exhibits diminished inducibility and increased susceptibility to CLA. These findings highlight the regulatory importance of the *uORF* in *M. abscessus* in the context of *whiB7* regulation.

The central role of the *uORF* in the regulation of a mycobacterial WhiB7 stress response

WhiB7 proteins are conserved transcriptional factors among *Actinomycetes*, likely serving as a self-defense mechanism against antibiotics produced by other soil bacteria (55). In mycobacteria, WhiB7 functions as an auto-regulatory transcriptional regulator involved in the activation of intrinsic multidrug resistance mechanisms (49, 50, 52). WhiB7 orchestrates the expression of over 100 genes, including those encoding the Tap drug efflux pump, the Eis acetyltransferase, the Erm ribosomal RNA methyltransferase, and the HflX ribosome splitting factor (39, 49, 56). This self-defense mechanism has been retained in pathogenic mycobacteria, such as *M. tuberculosis* and *M. abscessus*, where it is of pivotal importance for the antibiotic stress response (57). Despite the high conservation of *whiB7* within mycobacteria, the regulon of *whiB7* differs significantly between different mycobacterial species. In *M. abscessus*, *MAB_3508c* shows 75% identity to the *M. tuberculosis* gene *Rv3197A* (*whiB7*), yet the regulons are markedly different (39). A notable distinction between *MAB_3508c* and its *M. tuberculosis* counterpart is the former's reduced inducibility by AMK (39). Interestingly, *MAB_3508c* itself induces the expression of *eis2*, a gene absent in *M. tuberculosis*, which confers CLA-induced AMK resistance exclusively in *M. abscessus* (38, 39).

The regulation of gene expression represents a fundamental bacterial response to various stress conditions, including antibiotic exposure (58). Transcription attenuation structures, typically found adjacent to regulatory genes, often involve 5' UTR premature transcriptional terminator structures that prevent downstream gene transcription. For *whiB7*, a *uORF*-dependent transcriptional attenuation mechanism is believed to be conserved across *Actinomycetes* as demonstrated in *Streptomyces coelicolor* and *M. smegmatis* (40). In the absence of stress, transcription of *whiB7* commences from a distal upstream site. It subsequently progresses through a short *uORF*, thereby forming a Rho-independent terminator (RIT) that arrests transcription before reaching the *whiB7* ORF. During translation stress, such as exposure to macrolide antibiotics, inefficient translation of the *uORF* allows the formation of an antiterminator structure (**Figure S2**), which enables transcriptional

readthrough into the *whiB7* ORF. The presence of a WhiB7 binding site on the promoter of WhiB7 results in the formation of a positive feedback loop, which significantly amplifies *whiB7* levels and expression of its target genes (40, 49).

Although the WhiB7 regulatory mechanism is thought to be conserved across mycobacteria (40), the *uORF* displays limited sequence conservation among mycobacterial species (49), indicating that not all mycobacterial *whiB7* orthologs harbor similar stalling mechanisms. In *M. abscessus*, the *uORF* is notably distinct from those in other species, yet it shares some conserved nucleotide sequences present upstream of other *whiB7* orthologs (**Figure 4**). These variations may contribute to differential regulation of stress responses and resistance mechanisms, underscoring the complexity and variability of antibiotic resistance within the *Mycobacterium* genus.

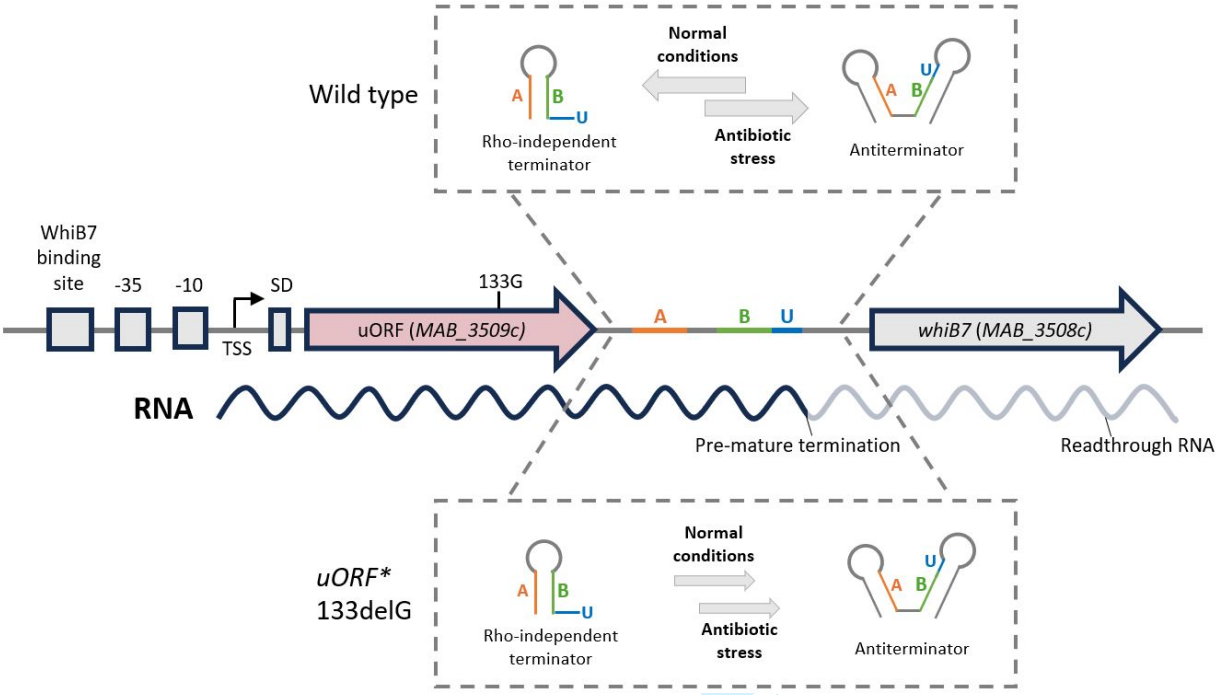

Figure 4. Proposed mechanism of the upstream *M. abscessus whiB7* sequence. Schematic representation of the upstream sequence of *M. abscessus whiB7*, illustrating a proposed regulatory mechanism: in the wild-type strain, a Rho-independent terminator, composed of a G-C stem-loop formed by base pairing between regions A (orange) and B (green), followed by a uridine tail (U region, blue), forms under normal conditions. This leads to premature transcription termination upstream of *whiB7* (black-lined RNA). In the presence of antibiotic stress, the RIT stem-loop is disrupted, allowing the formation of an antiterminator structure that facilitates RNA read-through and subsequent *whiB7* transcription (gray-lined RNA). In the *uORF** 133Gdel mutant, this regulatory mechanism is disrupted, favoring the formation of an antiterminator structure, even under non-stressed conditions. This ultimately leads to constitutive *whiB7* transcription. For clarity, the orientation of *MAB_3508c* and *MAB_3509c*, located on the minus strand of the *M. abscessus* ATCC19977 reference genome, has been reversed in this representation.

As illustrated in **Figure 4**, the *M. abscessus* upstream region of *whiB7* includes conserved nucleotide sequences essential for *whiB7* regulation (40). We identified a RIT structure, comprising a G-C loop followed by a uridine tail. In the absence of stress, this RIT sequence folds into a secondary structure that causes the RNA polymerase to pause and dissociate from the DNA template, resulting in a premature termination of transcription before the downstream gene is transcribed. However, in the presence of antibiotic stress, an antiterminator structure is formed, which prevents the formation of the RIT hairpin loop by adopting an alternative RNA secondary structure. This alternative structure permits the RNA polymerase to circumvent the termination signal, thus enabling the continued transcription of the downstream gene (59).

The precise mechanisms governing the switch from terminator to antiterminator switch in the induction of the Whib7 stress response remains unclear. Evidence from *M. smegmatis* and *M. tuberculosis* suggests that ribosome stalling by ribosome-targeting antibiotics may play a role, although alternative mechanisms, such as regulatory peptides, cannot be excluded (49, 60). In the absence of stress, these antiterminator-forming regions are stabilized by more distant stem-loop structures, which favors the formation of the terminator structure and premature transcription termination (61). Our *uORF**, located in an GC-rich upstream region of the RIT, likely destabilizes the GC-loop structures neighboring the antiterminator, favoring its formation over the terminator loop-stems. This results in enhanced transcriptional readthrough into the *whiB7* ORF, thereby promoting elevated *whiB7* expression and antibiotic resistance (**Figure 4**).

Mutations in clinical isolates could impact *whiB7* regulation and drug sensitivity.

In *M. tuberculosis*, mutations in *whiB7* and its upstream region result in both antibiotic resistance and sensitivity, depending on their location and the type of mutation (51, 53, 54). Our *in silico* analysis of 70 *M. abscessus abscessus* genomes revealed that strains of this subspecies carry mutations in proposed regulatory elements, more specifically at the WhiB7 binding site (G>A, position –487), at the transcription start site (TSS) (A>G, position –420), and upstream of the antiterminator (A>G, position –160). Conversely, analysis of 120 *M. abscessus massiliense* isolates demonstrated two conserved SNVs in GC-rich regions upstream of the hypothesized antiterminator (C>G, positions –260 and –286) and a conserved insertion near the transcription start region (position –425). Generally, *M. abscessus massiliense* exhibits higher treatment success rates due to its macrolide susceptibility. However, increased susceptibility is frequently attributed to a dysfunctional *erm(41)* gene (18).

Further investigation and molecular efforts are required to elucidate the precise effects of these mutations on *whiB7* expression in *M. abscessus* and the associated stress response. This is necessary to ascertain their predictive value in a clinical setting. As the process of sequencing becomes more accessible and integrated into clinical practice, and knowledge is expanding from other pathogenic mycobacteria, analyzing the *uORF* of *whiB7* could provide critical insights into the effectiveness of treatment strategies. This knowledge may facilitate the development of more personalized and effective approaches for the management of NTM-PD.

Utilizing the *uORF mutant as a tool strain in a *M. abscessus* drug discovery matrix**

The urgent need for novel therapeutic strategies for *M. abscessus* is highlighted by the restricted efficacy of existing treatment regimens (14). The discrepancy between the results of *in vitro* assays and the observed clinical outcomes represents a significant challenge (62). Individual assays provide limited support for *in vitro/in vivo* correlations. Therefore, using multiple assays in a screening matrix is considered a more reliable method (63). Recent advancements, such as the development of persister and biofilm assays utilizing the biofilm forming *M. abscessus bamboo* isolate strain, as well as the incorporation of clinical isolate panels, have greatly improved the process of discovering new drugs for *M. abscessus* (63).

In light of the anticipated reliance on macrolides and aminoglycosides in future *M. abscessus* regimens (15), the *uORF** mutant could prove a valuable addition to drug discovery matrixes. This mutant exhibits a WhiB7 stress response that mimics the stress responses induced by antibiotics in currently used treatment regimens. Consequently, it permits the screening of extensive compound libraries to identify molecules that circumvent the WhiB7-mediated stress response without the necessity of incorporating external stressors, such as CLA, into the assay. The latter would increase complexity and reduce scalability. Additionally, it could facilitate the assessment of new drug

candidates in combination with existing antibiotics, thereby providing a model for identifying compounds that can overcome or synergize with the stress-response mechanisms.

Moreover, it is important to validate the targets of novel drug candidates identified in screening efforts by investigating how these compounds interact with the stress-response pathways and whether they directly inhibit WhiB7 or its downstream effectors. This approach could help advance the development of efficacious treatments for *M. abscessus* infections via the use of the *uORF** mutant, potentially in conjunction with the *ΔuORF* mutant, to facilitate comprehensive mechanistic investigations.

Conclusion and future perspectives

Our findings highlight the pivotal role of the upstream regulatory region of *whiB7* in modulating its expression and subsequent antibiotic resistance. The stabilization of an antiterminator sequence in our mutant provides a potential mechanistic explanation for the observed elevated expression levels and resistance phenotypes. These insights into the regulatory mechanisms controlling *whiB7* expression may inform the development of novel therapeutic strategies aimed at overcoming intrinsic drug resistance in *M. abscessus*. Targeting the *uORF* and its regulatory elements may facilitate the development of novel therapeutic strategies. For example, the generation of drugs that are specifically designed to disrupt the formation of the antiterminator structure could potentially prevent upregulation of *whiB7* and its associated resistance genes. This approach could enhance the efficacy of existing antibiotics by mitigating the intrinsic resistance mechanisms of mycobacteria.

Further studies are needed to unravel the precise molecular mechanisms underlying WhiB7 regulation. Additional experiments such as developing WhiB7-reporter assays and performing genome-wide association studies on the growing repository of WGS data could provide valuable evidence for the clinical relevance of mutations in this upstream region and further clarify their contribution to drug resistance. These regulatory pathways may also present novel therapeutic targets, offering opportunities to enhance the efficacy of both current and future antibiotic regimens against *M. abscessus*. Thorough understanding of these regulatory mechanisms will facilitate the development of more effective treatments and improve clinical outcomes for patients suffering from NTM-PD.

Acknowledgements

We thank Johnson & Johnson for providing the resources needed to conduct this work. We extend our gratitude to Clara Aguilar Perez, Dirk Lamprecht, and the other members of the tuberculosis discovery team for their valuable discussions. Special thanks to Ronald de Hoogt, Carl Van Hove and Bram Van den Bergh for their assistance with sequencing, and to Sarah Megens for her experimental support.

We are grateful for the clinical isolate genomes made available through Johnson & Johnson. Our sincere thanks to our collaborators for providing the clinical isolates: Dr. Nicole Parrish from Johns Hopkins University (JHU, United States), Professor Satochi Mitarai from the Research Institute for Tuberculosis (RIT, Japan), and Professor Alexandra Aubry from Sorbonne University in France.

NDB is an employee of Vlaams Instituut voor Biotechnologie (VIB) and has received funding from Johnson & Johnson as well as from the Flanders Innovation & Entrepreneurship organization (VLAIO, HBC.2020.2202) for this work. This research was also supported by grants PRE2020-096507, awarded to EC-Y, and PID2019-104690RB-I00, awarded to JG-A, both funded by MCIN/AEI (10.13039/501100011033). Additionally, JM received support from the Research Foundation

Flanders (FWO) (G0B0420N), EOS - Excellence of Science (40007496), KU Leuven (C1 C16/23/007), and VIB.

Conflict of interest

The following authors were employees of Johnson & Johnson (the sponsor of the work) at the time when the described work was performed, and may hold Johnson & Johnson shares: CV, PTB, CV, NL, KT.

Data availability

The data underlying this article will be shared on reasonable request to the corresponding author.

Supplementary data

Table S1. Allelic exchange substrate (AES) for creating a *MAB_3509c* Zeocin knockout.

AES part	Nucleotide sequence
Homologous left arm (1000 bp)	GGCGGCATTCCGCCGGAGTTCGGCGAGGTGCTGTGCTGGGCGCGCGATGAGCAGTGGGACCAGGTGATCC GTCTGATCAAGCAGCTCGGCTTCATGCCGCCGGACGTTCAGCTGTCCGGGGATCAGGTGATGGATTACATCA GACCGCTTTGGCCCTATGTCGATCCGCTGCGCGCGGGTGAGTTCCATTTCACCCGCGAGTGGTTCCAGCAGG CCGCAGTCGCGTCGACCGACCTGTTGGACGAGGGATTCGCGGACCGATTCAAATTGGCGCGTCAGATGACG GTGCCGCCGGGTTACGTCATGCTGCTGCGCACTCTCGGCGGCATGATCGGGGTTCTGGTGCAACTCGATGC GCATGTGAACTACGCGGCGATCGCCGAACAATGGATGCCGGGATTCTTCCCGCCTAACTCCACATCGGCCTA AACGCATTGCTCCCCATCGCCGAATGACGATGGGGAGCAATGGTTATCAGGCCCTACAACCTTCTTGGCCGG CGGCGTCATGCCGCGGCGGTGTCGGCGTCGGGCAGTGGGTTCTTGCGCGGGCGTCCACGCGGCCGCTTGC GCGCCACAATGGTCCCCTGCTCAAGAATCTCACCGCCCCACACTCCCCACGGCTCTGCGCGGTCCAGCGCAG CGGCCAGGCACTGCGACCGGATCGGGCAGTCCGCGCACAGCGCCTTCGCCCGCTCCAGGTCGGCGGGGCTT TCCGCGAACCACAGGTCCGCGTCCGCGACGTGGCACGGCAGCGCGAGTCTTCGGGCCTCCACTTCAACGGT CATCATGTGTCCGTTCACCTGCTTCCTCTTCGGTTCCTCGTAAAACTGCTGGTCTCGTATCGGTGTCTTATCGA TCGAGATCCGGAACCACGCTTGAGGTTTGGGGCTCAAACAAATGTGGCCACGGATCCCGGTGGTGTCGGGT CCGTGGCCTGGGAGGCGGTTGTGGGGATACCTAGATGTATCCCCTATTCACGGACGCGACATTCGCGGCTG
Zeocin resistance cassette (700 bp)	GTGTAGGCTGGAGCTGCTTCGAAGTTCCTATACTTTCTAGAGAATAGGAACTTCGGAATAGGAACTTGTTGA CAATTAATCATCGGCATAGTATATCGGCATAGTATAATACGACAAGGTGAGGAACTAAACCATGGCCAAGTT GACCAGTGCCGTTCCGGTGCTCACCGCGCGCGACGTCGCCGGAGCGGTCGAGTTCTGGACCGACCGGCTCG GGTTCTCCCGGGACTTCGTGGAGGACGACTTCGCCGGTGTGGTCCGGGACGACGTGACCCTGTTCATCAGC GCGGTCCAGGACCAGGTGGTGCCGGACAACACCCTGGCCTGGGTGTGGGTGCGCGGCCTGGACGAGCTGT ACGCCGAGTGGTCGGAGGTCGTGTCCACGAACTTCCGGGACGCCTCTGGGCCGGCCATGACCGAGATCGGC GAGCAGCCGTGGGGGCGGGAGTTCGCCCTGCGCGACCCGGCCGGCAACTGCGTGCACTTCGTGGCCGAGG AGCAGGACTGAATGCATCTCTCCCCATGCGAGAGTAGGGAACTGCCAGGCATCAAATAAAACGAAAGGCTC AGTCGAAAGACTGGGCCTTTCGTTTTATCTGTTGTTTGTCGGTGAACGCTCTCCTGAGTAGGACAAATGAAGT TCCTATACTTTCTAGAGAATAGGAACTTCGGAATAGGAACTAAGGAGGATATTCATATG
Homologous right arm (1000 bp)	ATGGGCATCACGCCACAAGGTGTCTCCGTAATTGGTGGGTGTGTTCATTTCGCTCCTCCTTCCGTCTACTCGC ACGTGAACAGGTCTTGGTTTGGAATCCTCGCGAATTCCTGAAGCCCAGAGTAAAAGGTCACCTATCGGTTGA CAAGTTATTTTTGACCTGCGGCGATACTTCAAAACCAGTTTCGTCGAACTGGCATCTTTTCTCGGTGAGACAT GGCCGAAGATCAGCGGTGGCCCACCCTGGCACCGAAATCAACGTTGTGCAGATGCGCACTCACACTTTCCCT GCACAACGTCGATCTAGACATACTGGGCTCTACACGGAAGTGAGCAGCCGCGAGCGGAAAAGATCCAACAC CTGGTCGAGGGCCGCCCGTGTGGGCTGCCCGGGCTCATCGATGAGATGTTCGGTCACCACCGAGTGCGGCG GCATCGGCGAACCAGGACGAGCGGACTCACCGGGCAGCTCGATTGCAATGAACGCGTCCCCCAGTTCGTCG CGCAGGAACTGAAAACGCTCGGCGGGCACCAGTTTGTCGGTGGTGAAGCGCATGCCGATCACCTTGAGCCC CTCATGCTGGCAGCGGTGCTTGACCTTGCTCAGGTCCTCCGGAGAGATATCGATGTTGTACCGGGCCTTCTT ACTGAGGCCGAACGGTAGCGAGGGCTGCGACAGCACCGGTGCGAGCAGCCTGTCGTCTGCCGCCATGGCC AGCGCGTATCCACCGGTGAAACACATGCCGATGGCACCGACCCCCGGGCCGCCGTTGCGCTCATGTTCGTTC TGCGCCAGCGCCCGCAGCCAGTTGATCACCGACGAGGTCTTCCCCGTCGCCAGCACCGTAAATTCGCGGCTC ACGCATCCCCGGAACATCGAAGACGCCATGTAGGTGCTGGTACGCAGCCAACCATCGGCCTTCGGGTCGAC GCTTTGGCCGGGATTCCCGAAGAGGTGCGGCATGACGGCGGTGCAACCGATATCAGCCACCTTGCGCGC

Table S2. List of primers used in this study.

Primer name	Nucleotide sequence 5'-3'
***MAB_3509c* knockout**	
PCR-ZEO-FW	TGCGAGAGTAGGGAACTGCCAG
PCR-ZEO-RV	ACTGGTCAACTTGGCCATGGTT
PCR-3509C-FW	TTCTTTGTACCGGCGGTTGTCG
PCR-3509C-RV	GGGTGAAACCAAGATCGTATTGCGAAA
***rpoB* sequencing**	
PCR-RPOB-FW	TCCTGCCCACCTTCCCTC
PCR-RPOB-RV	GCTGGTTAGGCGAAGTCCTC
SANGER-RPOB-RRDR-FW	GGCCAGACCACGATGACC
SANGER-RPOB-RRDR-RV	GGCGAACCAGGATCTTCTCC
RT-qPCR	
qPCR-whiB7-FW	ACCTCAAGCGTGGTTCCG
qPCR-whiB7-RV	CCTCCACTTCAACGGTCATC
qPCR-AAC-FW	CTGTGTCCAATATGCCAACC
qPCR-AAC-RV	GAATGCCTCAATGAGTAATTCAC
qPCR-ERM-FW	GGAGTTCGTTGTGGATCTGG
qPCR-ERM-RV	AAACCGTGAACGAAGGTGTC
qPCR-EIS2-FW	GAGGTCAACCGCAAATTCAC
qPCR-EIS2-RV	CACGACATGACGGCTGAAC
qPCR-SIGA-FW	CACAAAGGGTTACAAGTTCTCG
qPCR-SIGA-RV	GCTTGTTGATGACCTCGACC

Table S3. Mean percentage of bacterial survival relative to the starting inoculum, determined at day 7 of each treatment round during the experimental evolution of *M. abscessus* under combined AMK and RFB pressure.

	Survival % day 7	**% increase relative to round 1**
Round 1	0.0182%	
Round 2	0.0209%	14.6%
Round 3	0.0854%	368.6%
Round 4	0.5078%	2687.2%

A NOVEL RESISTANCE-COFERRING MUTATION IN *M. ABSCESSUS*

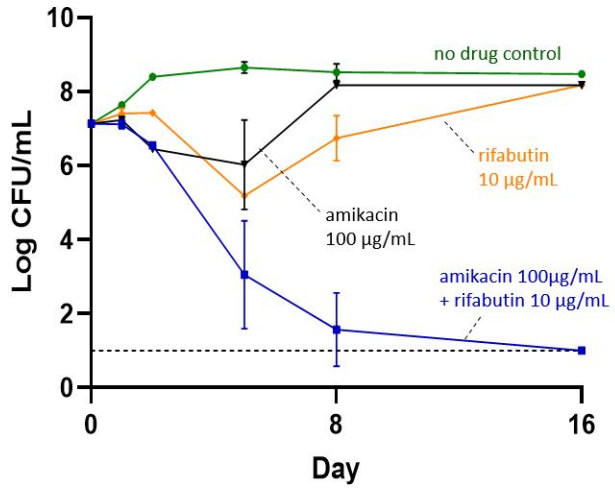

Figure S1. Colony-forming unit (CFU) enumeration. Blue: combination drug pressure of amikacin (100 µg/mL) and rifabutin (10 µg/mL), black: amikacin (100 µg/mL), orange: rifabutin (10 µg/mL), green: no drug growth control. The rapid regrowth observed under single-drug exposure highlights the emergence of resistance, while combination therapy effectively prevents the development of resistance.

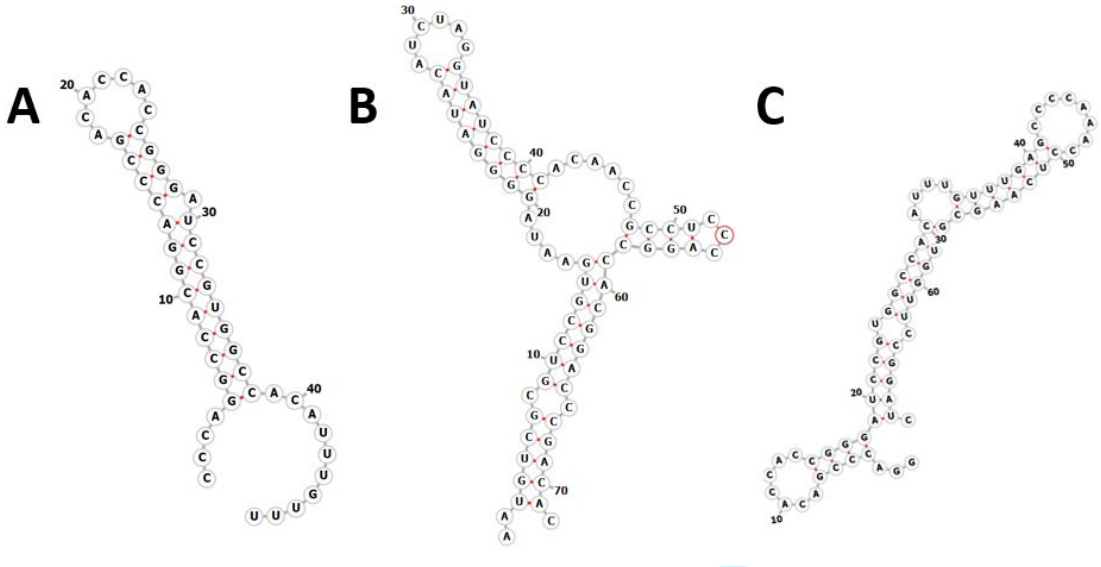

Figure S2. Predicted regulatory RNA fold loop structures constructed with RNA fold Vienna web server. (A) Predicted Rho-independent terminator structure at position –151 to –105 relative to the *whiB7* start codon. (B) Predicted upstream antiterminator structure at position –203 and –132 relative to the *whiB7* start codon. (C) Predicted downstream antiterminator structure at position –142 to –74 relative to the *whiB7* start codon.

References

1. Murray CJL, Ikuta KS, Sharara F, Swetschinski L, Aguilar GR, Gray A, Han C, Bisignano C, Rao P, Wool E, Johnson SC, Browne AJ, Chipeta MG, Fell F, Hackett S, Haines-Woodhouse G, Hamadani BHK, Kumaran EAP, McManigal B, Achalapong S, Agarwal R, Akech S, Albertson S, Amuasi J, Andrews J, Aravkin A, Ashley E, Babin F-X, Bailey F, Baker S, Basnyat B, Bekker A, Bender R, Berkley JA, Bethou A, Bielicki J, Boonkasidecha S, Bukosia J, Carvalheiro C, Castañeda-Orjuela C, Chansamouth V, Chaurasia S, Chiurchiù S, Chowdhury F, Donatien RC, Cook AJ, Cooper B, Cressey TR, Criollo-Mora E, Cunningham M, Darboe S, Day NPJ, Luca MD, Dokova K, Dramowski A, Dunachie SJ, Bich TD, Eckmanns T, Eibach D, Emami A, Feasey N, Fisher-Pearson N, Forrest K, Garcia C, Garrett D, Gastmeier P, Giref AZ, Greer RC, Gupta V, Haller S, Haselbeck A, Hay SI, Holm M, Hopkins S, Hsia Y, Iregbu KC, Jacobs J, Jarovsky D, Javanmardi F, Jenney AWJ, Khorana M, Khusuwan S, Kissoon N, Kobeissi E, Kostyanev T, Krapp F, Krumkamp R, Kumar A, Kyu HH, Lim C, Lim K, Limmathurotsakul D, Loftus MJ, Lunn M, Ma J, Manoharan A, Marks F, May J, Mayxay M, Mturi N, Munera-Huertas T, Musicha P, Musila LA, Mussi-Pinhata MM, Naidu RN, Nakamura T, Nanavati R, Nangia S, Newton P, Ngoun C, Novotney A, Nwakanma D, Obiero CW, Ochoa TJ, Olivas-Martinez A, Olliaro P, Ooko E, Ortiz-Brizuela E, Ounchanum P, Pak GD, Paredes JL, Peleg AY, Perrone C, Phe T, Phommasone K, Plakkal N, Ponce-de-Leon A, Raad M, Ramdin T, Rattanavong S, Riddell A, Roberts T, Robotham JV, Roca A, Rosenthal VD, Rudd KE, Russell N, Sader HS, Saengchan W, Schnall J, Scott JAG, Seekaew S, Sharland M, Shivamallappa M, Sifuentes-Osornio J, Simpson AJ, Steenkeste N, Stewardson AJ, Stoeva T, Tasak N, Thaiprakong A, Thwaites G, Tigoi C, Turner C, Turner P, Doorn HR van, Velaphi S, Vongpradith A, Vongsouvath M, Vu H, Walsh T, Walson JL, Waner S, Wangrangsimakul T, Wannapinij P, Wozniak T, Sharma TEMWY, Yu KC, Zheng P, Sartorius B, Lopez AD, Stergachis A, Moore C, Dolecek C, Naghavi M. 2022. Global burden of bacterial antimicrobial resistance in 2019: a systematic analysis. The Lancet 399:629–655.

2. Global Tuberculosis Report 2023. https://www.who.int/teams/global-tuberculosis-programme/tb-reports/global-tuberculosis-report-2023. Retrieved 12 November 2023.

3. Ratnatunga CN, Lutzky VP, Kupz A, Doolan DL, Reid DW, Field M, Bell SC, Thomson RM, Miles JJ. 2020. The Rise of Non-Tuberculosis Mycobacterial Lung Disease. Front Immunol 11.

4. Johansen MD, Herrmann J-L, Kremer L. 2020. Non-tuberculous mycobacteria and the rise of *Mycobacterium abscessus*. Nat Rev Microbiol 18:392–407.

5. Honda JR, Virdi R, Chan ED. 2018. Global Environmental Nontuberculous Mycobacteria and Their Contemporaneous Man-Made and Natural Niches. Front Microbiol 9:2029.

6. Prieto MD, Alam ME, Franciosi AN, Quon BS. 2023. Global burden of nontuberculous mycobacteria in the cystic fibrosis population: a systematic review and meta-analysis. ERJ Open Res 9:00336.

7. Prevots DR, Marras TK. 2015. Epidemiology of Human Pulmonary Infection with Non-Tuberculous Mycobacteria: A Review. Clin Chest Med 36:13–34.

8. Strnad L, Winthrop K. 2018. Treatment of *Mycobacterium abscessus* Complex. Semin Respir Crit Care Med 39:362–376.

9. Yang J-H, Wang P-H, Pan S-W, Wei Y-F, Chen C-Y, Lee H-S, Shu C-C, Wu T-S. 2022. Treatment Outcome in Patients with *Mycobacterium abscessus* Complex Lung Disease: The Impact of Tigecycline and Amikacin. Antibiotics 11:571.

10. Daley CL, Iaccarino JM, Lange C, Cambau E, Wallace RJ Jr, Andrejak C, Böttger EC, Brozek J, Griffith DE, Guglielmetti L, Huitt GA, Knight SL, Leitman P, Marras TK, Olivier KN, Santin M, Stout JE, Tortoli E, van Ingen J, Wagner D, Winthrop KL. 2020. Treatment of Nontuberculous

Mycobacterial Pulmonary Disease: An Official ATS/ERS/ESCMID/IDSA Clinical Practice Guideline. Clin Infect Dis 71:e1–e36.

11. Kwak N, Dalcolmo MP, Daley CL, Eather G, Gayoso R, Hasegawa N, Jhun BW, Koh W-J, Namkoong H, Park J, Thomson R, Ingen J van, Zweijpfenning SMH, Yim J-J. 2019. *Mycobacterium abscessus* pulmonary disease: individual patient data meta-analysis. Eur Respir J 54:1801991.

12. Pasipanodya JG, Ogbonna D, Ferro BE, Magombedze G, Srivastava S, Deshpande D, Gumbo T. 2017. Systematic Review and Meta-analyses of the Effect of Chemotherapy on Pulmonary *Mycobacterium abscessus* Outcomes and Disease Recurrence. Antimicrob Agents Chemother 61:10.1128/aac.01206-17.

13. Luthra S, Rominski A, Sander P. 2018. The Role of Antibiotic-Target-Modifying and Antibiotic-Modifying Enzymes in *Mycobacterium abscessus* Drug Resistance. Front Microbiol 9:2179.

14. Lopeman RC, Harrison J, Desai M, Cox JAG. 2019. *Mycobacterium abscessus*: Environmental Bacterium Turned Clinical Nightmare. 3. Microorganisms 7:90.

15. Schildkraut JA, Coolen JPM, Burbaud S, Sangen JJN, Kwint MP, Floto RA, op den Camp HJM, te Brake LHM, Wertheim HFL, Neveling K, Hoefsloot W, van Ingen J. 2022. RNA Sequencing Elucidates Drug-Specific Mechanisms of Antibiotic Tolerance and Resistance in *Mycobacterium abscessus*. Antimicrob Agents Chemother 66:e01509-21.

16. Stout JE, Floto RA. 2012. Treatment of *Mycobacterium abscessus*. Am J Respir Crit Care Med 186:822–823.

17. Bastian S, Veziris N, Roux A-L, Brossier F, Gaillard J-L, Jarlier V, Cambau E. 2011. Assessment of Clarithromycin Susceptibility in Strains Belonging to the *Mycobacterium abscessus* Group by *erm(41)* and *rrl* Sequencing. Antimicrob Agents Chemother 55:775–781.

18. Richard M, Gutiérrez AV, Kremer L. 2020. Dissecting *erm(41)*-Mediated Macrolide-Inducible Resistance in *Mycobacterium abscessus*. Antimicrob Agents Chemother 64:e01879-19.

19. Rominski A, Roditscheff A, Selchow P, Böttger EC, Sander P. 2017. Intrinsic rifamycin resistance of *Mycobacterium abscessus* is mediated by ADP-ribosyltransferase MAB_0591. J Antimicrob Chemother 72:376–384.

20. Schäfle D, Selchow P, Borer B, Meuli M, Rominski A, Schulthess B, Sander P. 2021. Rifabutin Is Inactivated by *Mycobacterium abscessus* Arr. Antimicrob Agents Chemother 65:e02215-20.

21. Goh BC, Larsson S, Dam LC, Ling YHS, Chua WLP, Abirami R, Singh S, Ong JLE, Teo JWP, Ho P, Ingham PW, Pethe K, Dedon PC. 2023. Rifaximin potentiates clarithromycin against *Mycobacterium abscessus* in vitro and in zebrafish. JAC-Antimicrob Resist 5:dlad052.

22. Henriette Zweijpfenning SM, Chiron R, Essink S, Schildkraut J, Akkerman OW, Aliberti S, Altenburg J, Arets B, van Braeckel E, Delaere B, Gohy S, Haarman E, Lorent N, McKew G, Morgan L, Wagner D, van Ingen J, Hoefsloot W. 2022. Safety and Outcomes of Amikacin Liposome Inhalation Suspension for *Mycobacterium abscessus* Pulmonary Disease. Chest 162:76–81.

23. Raaijmakers J, Schildkraut JA, Hoefsloot W, Van Ingen J. 2021. The role of amikacin in the treatment of nontuberculous mycobacterial disease. Expert Opin Pharmacother 22:1961–1974.

24. Bollen C, Louwagie E, Verstraeten N, Michiels J, Ruelens P. 2023. Environmental, mechanistic and evolutionary landscape of antibiotic persistence. EMBO Rep 24:e57309.

25. Balaban NQ, Helaine S, Lewis K, Ackermann M, Aldridge B, Andersson DI, Brynildsen MP, Bumann D, Camilli A, Collins JJ, Dehio C, Fortune S, Ghigo J-M, Hardt W-D, Harms A, Heinemann M, Hung DT, Jenal U, Levin BR, Michiels J, Storz G, Tan M-W, Tenson T, Van Melderen L,

Zinkernagel A. 2019. Definitions and guidelines for research on antibiotic persistence. Nat Rev Microbiol 17:441–448.

26. Lewis K. 2010. Persister cells. Annu Rev Microbiol 64:357–372.

27. Jain P, Weinrick BC, Kalivoda EJ, Yang H, Munsamy V, Vilcheze C, Weisbrod TR, Larsen MH, O'Donnell MR, Pym A, Jacobs WR. 2016. Dual-Reporter Mycobacteriophages (Φ2DRMs) Reveal Preexisting *Mycobacterium tuberculosis* Persistent Cells in Human Sputum. mBio 7:e01023-16.

28. Torrey HL, Keren I, Via LE, Lee JS, Lewis K. 2016. High Persister Mutants in *Mycobacterium tuberculosis*. PLOS ONE 11:e0155127.

29. Quigley J, Lewis K. 2022. Noise in a Metabolic Pathway Leads to Persister Formation in *Mycobacterium tuberculosis*. Microbiol Spectr 10:e02948-22.

30. Boldrin F, Provvedi R, Cioetto Mazzabò L, Segafreddo G, Manganelli R. 2020. Tolerance and Persistence to Drugs: A Main Challenge in the Fight Against *Mycobacterium tuberculosis*. Front Microbiol 11:1924.

31. Lee CL, Ng HF, Ngeow YF, Thaw Z. 2021. A stop-gain mutation in sigma factor SigH (MAB_3543c) may be associated with tigecycline resistance in *Mycobacteroides abscessus*. J Med Microbiol 70:001378.

32. Richard M, Gutiérrez AV, Viljoen A, Rodriguez-Rincon D, Roquet-Baneres F, Blaise M, Everall I, Parkhill J, Floto RA, Kremer L. 2018. Mutations in the MAB_2299c TetR Regulator Confer Cross-Resistance to Clofazimine and Bedaquiline in *Mycobacterium abscessus*. Antimicrob Agents Chemother 63:e01316-18.

33. Bernard C, Liu Y, Larrouy-Maumus G, Guilhot C, Cam K, Chalut C. 2024. Altered serine metabolism promotes drug tolerance in *Mycobacterium abscessus* via a WhiB7-mediated adaptive stress response. Antimicrob Agents Chemother 0:e01456-23.

34. Troian EA, Maldonado HM, Chauhan U, Barth VC, Woychik NA. 2023. *Mycobacterium abscessus* VapC5 toxin potentiates evasion of antibiotic killing by ribosome overproduction and activation of multiple resistance pathways. Nat Commun 14:3705.

35. Mouton JW. 1999. Combination therapy as a tool to prevent emergence of bacterial resistance. Infection 27 Suppl 2:S24-28.

36. Dartois V, Dick T. 2024. Toward better cures for *Mycobacterium abscessus* lung disease | Clinical Microbiology Reviews. Clin Microbiol Rev.

37. Campos-Pardos E, Uranga S, Picó A, Gómez AB, Gonzalo-Asensio J. 2024. Dependency on host vitamin B12 has shaped *Mycobacterium tuberculosis* Complex evolution. Nat Commun 15:2161.

38. Pryjma M, Burian J, Kuchinski K, Thompson CJ. 2017. Antagonism between Front-Line Antibiotics Clarithromycin and Amikacin in the Treatment of *Mycobacterium abscessus* Infections Is Mediated by the *whiB7* Gene. Antimicrob Agents Chemother 61:e01353-17.

39. Hurst-Hess K, Rudra P, Ghosh P. 2017. *Mycobacterium abscessus* WhiB7 Regulates a Species-Specific Repertoire of Genes To Confer Extreme Antibiotic Resistance. Antimicrob Agents Chemother 61:e01347-17.

40. Lee J-H, Lee E-J, Roe J-H. 2022. uORF-mediated riboregulation controls transcription of *whiB7/wblC* antibiotic resistance gene. Mol Microbiol 117:179–192.

41. Gruber AR, Lorenz R, Bernhart SH, Neuböck R, Hofacker IL. 2008. The Vienna RNA Websuite. Nucleic Acids Res 36:W70–W74.

42. Nessar R, Reyrat JM, Murray A, Gicquel B. 2011. Genetic analysis of new 16S rRNA mutations conferring aminoglycoside resistance in *Mycobacterium abscessus*. J Antimicrob Chemother 66:1719–1724.

43. Johansen MD, Daher W, Roquet-Banères F, Raynaud C, Alcaraz M, Maurer FP, Kremer L. 2020. Rifabutin Is Bactericidal against Intracellular and Extracellular Forms of *Mycobacterium abscessus*. Antimicrob Agents Chemother 64:e00363-20.

44. Bonalsky JR, Jaconia D, Konopka EA, Adair FW. 1975. Analysis of Rifampin Disk Diffusion and Stability in 7H10 Agar. Antimicrob Agents Chemother 8:187–193.

45. Cooper KE, Linton AH, Sehgal SN. 1958. The Effect of Inoculum Size on Inhibition Zones in Agar Media Using Staphylococci and Streptomycin. J Gen Microbiol 18:670–687.

46. Ng HF, Ngeow YF. 2023. Mutations in Genes Encoding 23S rRNA and FadD32 May be Associated with Linezolid Resistance in *Mycobacteroides abscessus*. Microb Drug Resist Larchmt N 29:41–46.

47. Maurer FP, Rüegger V, Ritter C, Bloemberg GV, Böttger EC. 2012. Acquisition of clarithromycin resistance mutations in the 23S rRNA gene of *Mycobacterium abscessus* in the presence of inducible erm(41). J Antimicrob Chemother 67:2606–2611.

48. Johansen SK, Maus CE, Plikaytis BB, Douthwaite S. 2006. Capreomycin Binds across the Ribosomal Subunit Interface Using tlyA-Encoded 2′-O-Methylations in 16S and 23S rRNAs. Mol Cell 23:173–182.

49. Poulton NC, DeJesus MA, Munsamy-Govender V, Kanai M, Roberts CG, Azadian ZA, Bosch B, Lin KM, Li S, Rock JM. 2024. Beyond antibiotic resistance: The *whiB7* transcription factor coordinates an adaptive response to alanine starvation in mycobacteria. Cell Chem Biol 669–682.

50. Burian J, Thompson CJ. 2018. Regulatory genes coordinating antibiotic-induced changes in promoter activity and early transcriptional termination of the mycobacterial intrinsic resistance gene *whiB7*. Mol Microbiol 107:402–415.

51. Reeves AZ, Campbell PJ, Sultana R, Malik S, Murray M, Plikaytis BB, Shinnick TM, Posey JE. 2013. Aminoglycoside Cross-Resistance in *Mycobacterium tuberculosis* Due to Mutations in the 5' Untranslated Region of *whiB7*. Antimicrob Agents Chemother 57:1857–1865.

52. Geiman DE, Raghunand TR, Agarwal N, Bishai WR. 2006. Differential Gene Expression in Response to Exposure to Antimycobacterial Agents and Other Stress Conditions among Seven *Mycobacterium tuberculosis whiB* -Like Genes. Antimicrob Agents Chemother 50:2836–2841.

53. Li S, Poulton NC, Chang JS, Azadian ZA, DeJesus MA, Ruecker N, Zimmerman MD, Eckartt KA, Bosch B, Engelhart CA, Sullivan DF, Gengenbacher M, Dartois VA, Schnappinger D, Rock JM. 2022. CRISPRi chemical genetics and comparative genomics identify genes mediating drug potency in *Mycobacterium tuberculosis*. Nat Microbiol 7:766–779.

54. 2022. Genome-wide association studies of global *Mycobacterium tuberculosis* resistance to 13 antimicrobials in 10,228 genomes identify new resistance mechanisms. PLoS Biol 20:e3001755.

55. Bush MJ. 2018. The actinobacterial WhiB-like (Wbl) family of transcription factors. Mol Microbiol 110:663–676.

56. Hurst-Hess K, McManaman C, Yang Y, Gupta S, Ghosh P. 2023. Hierarchy and interconnected networks in the WhiB7 mediated transcriptional response to antibiotic stress in *Mycobacterium abscessus*. PLoS Genet 19:e1011060.

57. Davies-Bolorunduro OF, Jaemsai B, Ruangchai W, Phumiphanjarphak W, Aiewsakun P, Palittapongarnpim P. 2023. Analysis of *whiB7* in *Mycobacterium tuberculosis* reveals novel AT-hook deletion mutations. Sci Rep 13:13324.

58. Merino E, Yanofsky C. 2005. Transcription attenuation: a highly conserved regulatory strategy used by bacteria. Trends Genet 21:260–264.

59. Santangelo TJ, Artsimovitch I. 2011. Termination and antitermination: RNA polymerase runs a stop sign. Nat Rev Microbiol 9:319–329.

60. Kipkorir T, Polgar P, Barker D, D'Halluin A, Patel Z, Arnvig KB. 2024. A novel regulatory interplay between atypical B12 riboswitches and uORF translation in *Mycobacterium tuberculosis*. Nucleic Acids Res gkae338.

61. Millman A, Dar D, Shamir M, Sorek R. 2017. Computational prediction of regulatory, premature transcription termination in bacteria. Nucleic Acids Res 45:886–893.

62. Boeck L. 2023. Antibiotic tolerance: targeting bacterial survival. Curr Opin Microbiol 74:102328.

63. Wu M-L, Aziz DB, Dartois V, Dick T. 2018. NTM drug discovery: status, gaps and the way forward. Drug Discov Today 23:1502–1519.